

Article

Grassland Productivity and Ewes' Forage Intake Monitoring by Combined Multispectral Vegetation Indices and Machine Learning Approaches for Precision Grazing Management

Pasquale Caparra ¹, Salvatore Praticò ¹, Gaetano Messina ^{1,*}, Caterina Cilione ¹, Paolo De Caria ¹, Emilio Lo Presti ¹, Ada Braghieri ², Adriana Di Trana ², Rosanna Paolino ² and Giuseppe Badagliacca ¹

¹ Department AGRARIA, Mediterranean University of Reggio Calabria, Loc. Feo di Vito snc, 89122 Reggio Calabria, Italy; pasquale.caparra@unirc.it (P.C.); salvatore.pratico@unirc.it (S.P.); caterina.cilione@unirc.it (C.C.); paolo.decaria@unirc.it (P.D.C.); emilio.lopresti@unirc.it (E.L.P.); giuseppe.badagliacca@unirc.it (G.B.)

² Department of Agricultural, Forest, Food, and Environmental Sciences, University of Basilicata, 85100 Potenza, Italy; ada.braghieri@unibas.it (A.B.); adriana.ditrana@unibas.it (A.D.T.); rosanna.paolino@unibas.it (R.P.)

* Correspondence: gaetano.messina@unirc.it

Abstract

Grassland productivity and precise monitoring of animal herbage intake are key requirements for sustainable grazing management in Mediterranean upland systems. This study aimed to evaluate the potential of uncrewed aerial vehicle (UAV)-based multispectral vegetation indices (VIs) combined with machine learning (ML) algorithms to estimate forage biomass, quality parameters and daily herbage dry matter intake (HDMI) of grazing ewes at the paddock scale. The experiment was conducted in a managed ryegrass–white clover meadow–pasture in southern Italy, where four plots were grazed sequentially by lactating Sarda ewes during spring–summer 2025. Ground measurements included pre- and post-grazing biomass inside and outside exclusion cages, botanical composition and forage quality. Concurrently, UAV multispectral imagery has been acquired, from which several VIs were computed. Pearson's correlations were used to explore relationships between VIs and forage variables, and five ML algorithms. Indices such as MCARI2, MTVI2, MTVI, MSAVI and OSAVI showed the strongest associations with biomass and quality traits, while support vector machine and neural networks provided the best prediction accuracies, particularly for HDMI (R^2 up to 0.91). The integrated UAV–ML approach proved effective in simultaneously capturing spatial variability of pasture productivity and animal intake, supporting the development of operational precision grazing tools for heterogeneous Mediterranean grasslands.

Keywords: precision livestock farming (PLF); Sarda ewes; herbage dry matter intake (HDMI); remote sensing; grassland biomass; forage quality; sustainable pasture management



Academic Editor: Mark Altaweel

Received: 17 February 2026

Revised: 11 March 2026

Accepted: 13 March 2026

Published: 17 March 2026

Copyright: © 2026 by the authors.

Licensee MDPI, Basel, Switzerland.

This article is an open access article distributed under the terms and

conditions of the [Creative Commons](https://creativecommons.org/licenses/by/4.0/)

[Attribution \(CC BY\)](https://creativecommons.org/licenses/by/4.0/) license.

1. Introduction

Grasslands are among the most widespread land-use systems globally, providing essential ecosystem services, including livestock feed production, biodiversity conservation, carbon sequestration, and landscape stability, particularly in marginal and mountainous areas [1–3]. In Mediterranean upland regions, permanent grasslands are fundamental for sustaining extensive livestock systems and preserving high nature value landscapes, many of

which are located within protected areas [4–7]. These agro-pastoral systems are increasingly threatened by climate variability, land abandonment, and suboptimal grazing management, factors that can reduce forage productivity and compromise long-term sustainability [8,9].

Precision grazing management has gained attention as an effective strategy to optimise pasture utilization. By leveraging Precision Livestock Farming (PLF) technologies, such as GPS tracking, accelerometers, and remote sensing, farmers can monitor forage availability, sward quality, and livestock behaviour in real time. This enables alignment of grazing patterns with animals' nutritional requirements, minimises over- or under-grazing, and enhances grassland productivity and sustainability [10,11]. Accurate assessment of grassland productivity and animal herbage dry matter intake (HDMI) is a critical prerequisite for precision grazing. Traditional methods, based on destructive biomass sampling and exclusion cages, provide reliable estimates but are time-consuming, spatially limited, and difficult to scale for operational decision-making [12,13]. These limitations reduce applicability in dynamic grazing systems, where timely information is essential for adaptive management.

Remote sensing technologies offer non-destructive, spatially explicit, and repeatable monitoring of grassland conditions [14,15]. Uncrewed aerial vehicles (UAVs) equipped with multispectral sensors provide ultra-high spatial resolution data, suitable for heterogeneous grasslands at the paddock scale [16–18]. Multispectral vegetation indices (VIs) derived from visible, red-edge, and infrared bands have been widely applied to estimate herbage biomass, chlorophyll concentration, and key forage quality parameters, supporting precision grazing management [19–21]. However, the performance of individual VIs is influenced by botanical composition, phenological stage, and grazing pressure, especially in mixed grass–legume swards typical of Mediterranean mountain pastures [22].

Machine learning (ML) models offer a robust framework for modelling complex and nonlinear relationships between spectral data and grassland biophysical variables, often outperforming traditional linear regression in heterogeneous pastures [23–25]. Algorithms such as random forest (RF), support vector machines (SVM), k-nearest neighbours (k-NN), and neural networks (NN) have demonstrated superior performance in predicting herbage biomass and forage quality parameters from UAV-derived data [26,27]. Despite these advances, most studies focus primarily on vegetation-related variables, while direct estimation of animal HDMI under grazing conditions remains largely underexplored [28]. Addressing this gap is essential for developing spatially explicit, scalable tools linking pasture characteristics directly to animal responses, thereby supporting precision grazing management.

Herbage intake is a key determinant of animal performance and grazing system efficiency [29]. Conventional intake estimation methods, based on exclusion cages and pre- and post-grazing biomass measurements, remain reference approaches [30], but are rarely integrated with high-resolution remote sensing and advanced ML modelling techniques.

Within this context, the present study investigates the combined use of UAV-based multispectral VIs and ML models to monitor grassland productivity and estimate daily HDMI of grazing ewes in a Mediterranean upland pasture. The specific objectives were as follows: (i) evaluate the potential of multispectral indices as predictors of biomass and quality; and (ii) evaluate and compare different machine learning algorithms in terms of predictive accuracy, robustness, and potential generalizability for estimating herbage biomass and HDMI. The main novelty of this work lies in the simultaneous estimation of pasture productivity and animal herbage intake using high-resolution UAV data and ML models under operational grazing conditions, providing new insights into precision land management strategies for sustainable grasslands.

2. Materials and Methods

2.1. Experimental Site

The field experiment was conducted at the “Fattoria Biò” pilot farm located in Celico municipality (Cosenza, Calabria, Southern Italy) within the protected area of the Sila National Park (39° 23′ 33″ N, 16° 27′ 40″ E, 1177 m a.s.l.). The main soil properties, referred to the 0–20 cm layer, were as follows: clay 20.0%, silt 11.0% and sand 69.0%, sandy clay loam texture, pH 5.86 (1:2.5H₂O), organic matter 2.25%, C/N ratio 10.5, available P 24.8 mg kg⁻¹, exchangeable K 192.2 mg kg⁻¹ [31]. The soil is classified as a Humic Pachic Dystrudepts [32]. More detailed information regarding experimental soil is available in Cilione et al. [33].

The experimental site has a typical upland Mediterranean climate [34]. Based on long-term observations, the mean annual air temperature is 10.0 °C, with average annual minimum and maximum values of 4.3 °C and 16.2 °C, respectively. Sub-zero temperatures may occur for up to eight months of the year, from October to May. The mean annual precipitation amounts to 1634 mm, predominantly falling in autumn–winter and spring (October–March), whereas July and August are typically dry. During winter, snow cover persists on the ground for at least three months.

2.2. Experimental Design, Sampling and Analysis

The experimental activity was conducted in a meadow-pasture area covering about 1.0 hectares during spring-summer 2025. The area was ploughed and sown four years prior to the experiment with a grassland seed mixture composed of ryegrass (*Lolium perenne* L.) and white clover (*Trifolium repens* L.) at a 70:30 (*w/w*) ratio. Since its establishment, the site has been continuously managed under controlled sheep grazing and hay production practices, including periodic mowing and biomass baling. No fertilisation or other agronomic inputs have been applied during the entire management period. The field is typically utilised for grazing and forage harvesting from April to September.

At the beginning of the experiment, the meadow-pasture was divided into four plots (Figure 1), each covering about 0.25 ha, used sequentially for sheep grazing with an average stay of 8 days (Plot A: 03/06/2025–17/06/2025; Plot B: 17/06/2025–26/06/2025; Plot C: 26/06/2025–04/07/2025; Plot D: 04/07/2025–11/07/2025).

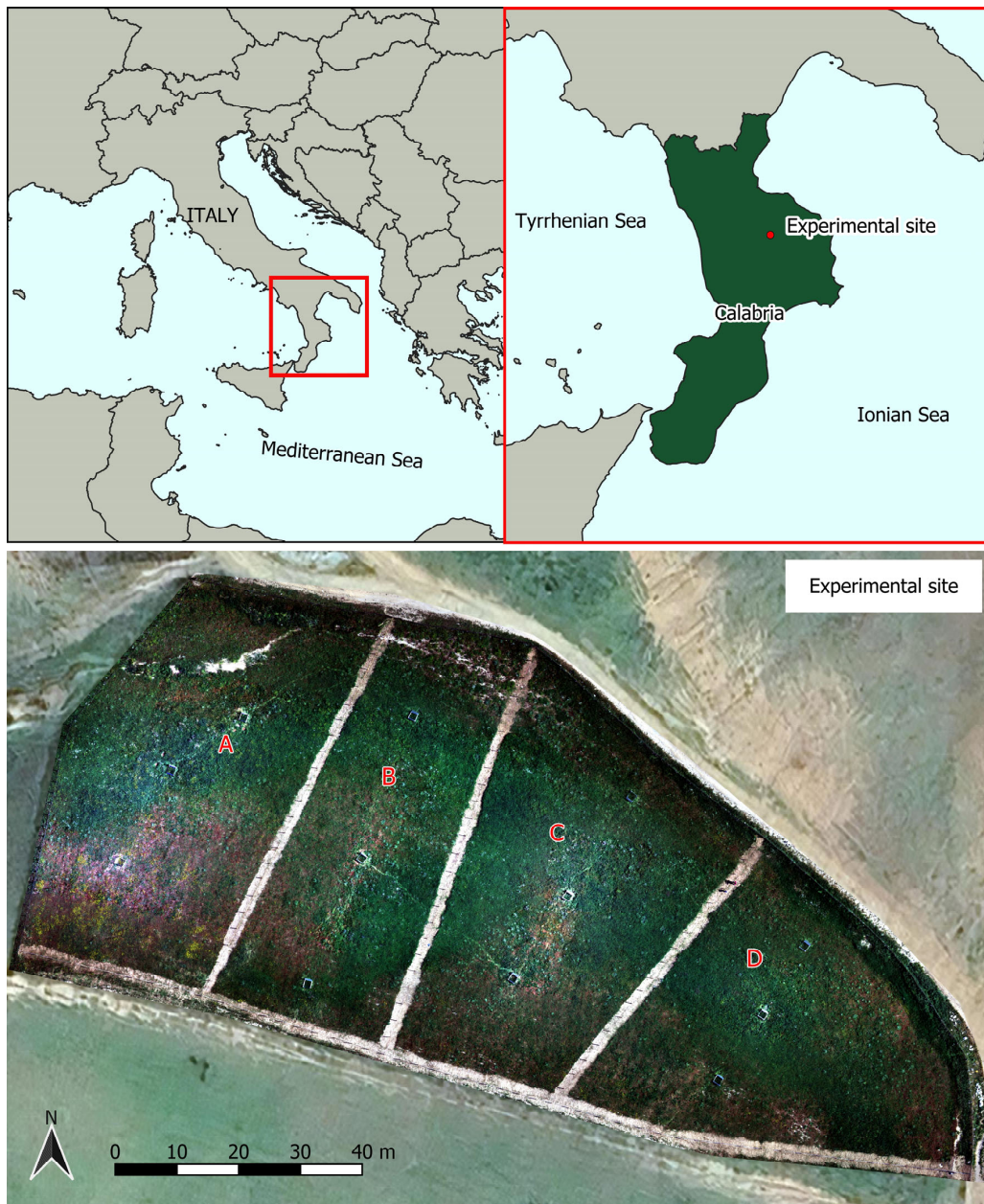


Figure 1. On the top is the location of the experimental site in the Celico municipality (Cosenza, Calabria, Southern Italy). On the bottom is the orthomosaic of the field with the experimental design (four plots named A-B-C-D).

2.3. Animals and Animal Management

The animal protocol and the implemented procedures described below were in accordance with the ethical guidelines in force at the University “Mediterranea” of Reggio Calabria, in full compliance with the European Union directive 2010/63/UE and the recommendation of the Commission of the European Communities 2007/526/EC. Twenty-four mature Sarda ewes were selected from the farm flock on the basis of similar lactation stage, milk production, live weight, and body condition score, and were included in the experimental trial. Animals were machine-milked twice daily at 07:00 a.m. and 03:00 p.m. On each experimental day, the ewes were led to their respective plots and grazed there from morning until afternoon (i.e., between the two milking sessions). Outside this grazing period, the animals were kept indoors and received a daily allowance of 400 g head⁻¹ of a commercial pelleted concentrate, provided in two equal meals at milking. Throughout the

housing period, ewes had ad libitum access to fresh water. All sheep remained in good health throughout the experimental period and were returned to their pre-experimental management conditions to resume normal husbandry after the trial.

2.4. Herbage Sampling and Analysis for Ground Truth Data Determination

In each plot, three square-based stainless steel exclusion cages (1.0 m × 1.0 m) were installed to assess herbage growth during the grazing period (Figure 2a). Forage biomass, within each plot, was sampled over a surface area of 1.0 m² before and after grazing by hand-cutting the vegetation to a stubble height of 0.02 m. At the beginning of the grazing period, samples were collected at three randomly selected points (herbage before), whereas at the end of grazing, biomass was sampled both inside the exclusion cages (herbage inside cage, HIC) and in the adjacent grazed areas (herbage external cage, HEC) (Figure 2b). To reduce sampling variability, all herbage mass samples were collected by the same trained operator using a single-handed reaping hook throughout the entire trial (Figure 2c). Overall, the sampling campaign resulted in a total of 36 herbage samples collected on five different dates (T0: 03/06/2025; T1: 17/06/2025; T2: 26/06/2025; T3: 04/07/2025; T4: 11/07/2025). The position of all sampling points has been surveyed by the Stonex S990 + GNSS receiver with an accuracy of ±2.5 cm in horizontal and ±5.0 cm in vertical, thanks to the possibility to get real time positioning corrections through the real-time kinematic (RTK) process.



Figure 2. On the left (a), one of the stainless steel exclusion cages placed in the study area. At the centre (b), biomass sampling inside and outside the cage using a single-handed reaping hook (c). Next (right (d)), the samples are collected in separate bags for transport to the analysis laboratory.

The harvested biomass was placed in plastic bags and promptly transported to the laboratory (Figure 2d). Fresh samples were then separated according to botanical family, distinguishing between cereals and legumes, while plant species not belonging to these two families were grouped into a “mixed” category. Then, the samples were oven-dried at 60 °C and ground using a laboratory mill (1 mm sieve) before further analysis. The dry matter (DM) of herbage was determined by drying samples at 105 °C in the forced-air oven until reaching constant weight. Ash content was determined by incineration in a muffle furnace at 550 °C for 12 h. Crude protein (CP) was quantified using the Kjeldahl method [35], calculating nitrogen content and applying a conversion factor of 6.25, while ether extract (EE) was determined by the Soxhlet extraction method [36]. Fibre fractions, including neutral detergent fibre (NDF), acid detergent fibre (ADF), and acid detergent lignin (ADL), were analysed following the procedure described by Van Soest et al. [37].

Daily mean herbage intake on DM basis (HDMI, $\text{g m}^{-2} \text{d}^{-1}$), according to Undi et al. [38], was calculated on herbage sampled after the grazing period, as follows (Equation (1)):

$$\text{HDMI} [\text{g m}^{-2} \text{d}^{-1}] = \frac{\text{HDMIC} [\text{g m}^{-2}] - \text{HDMEC} [\text{g m}^{-2}]}{D [\text{d}]} \quad (1)$$

where *HDMIC* is the herbage dry matter biomass inside the exclusion cage, *HDMEC* is the herbage dry matter biomass external in the proximity of the exclusion cage, and *D* is the grazing period duration in days (d).

2.5. UAV Surveys and Image Processing

At each sampling time (T0–T4), a multirotor DJI Phantom 4 Multispectral UAV (DJI Ltd., Shenzhen, China) was employed to conduct the multispectral survey (Figure 3a). The UAV is equipped with a 2 MP (1600×1300 pixels) camera capable of capturing five spectral bands in addition to RGB: Blue ($450 \text{ nm} \pm 16 \text{ nm}$), Green ($560 \text{ nm} \pm 16 \text{ nm}$), Red ($650 \text{ nm} \pm 16 \text{ nm}$), Red Edge ($730 \text{ nm} \pm 16 \text{ nm}$), and Near-Infrared (NIR— $840 \text{ nm} \pm 26 \text{ nm}$). Each survey was carried out at a flight speed of 2 m s^{-1} and an altitude of 40 m above ground level. Five geo-referenced ground control points (GCPs) were deployed across the field using the Stonex S990 + GNSS. Each GCP consisted of a $50 \times 50 \text{ cm}$ white polypropylene panel, with two quadrants covered in black cardboard to facilitate centre point identification (Figure 3b). Multispectral images were processed via aerial image triangulation using the geo-tagged flight log and GCP coordinates in Agisoft Metashape (Agisoft LLC, version 2.1.0, St. Petersburg, Russia). Figure 4 summarises the overall workflow for the UAV survey and image processing.



Figure 3. (a), DJI Phantom 4 Multispectral employed for aerial surveys. (b) Determination of the position of a ground control point (GCP).

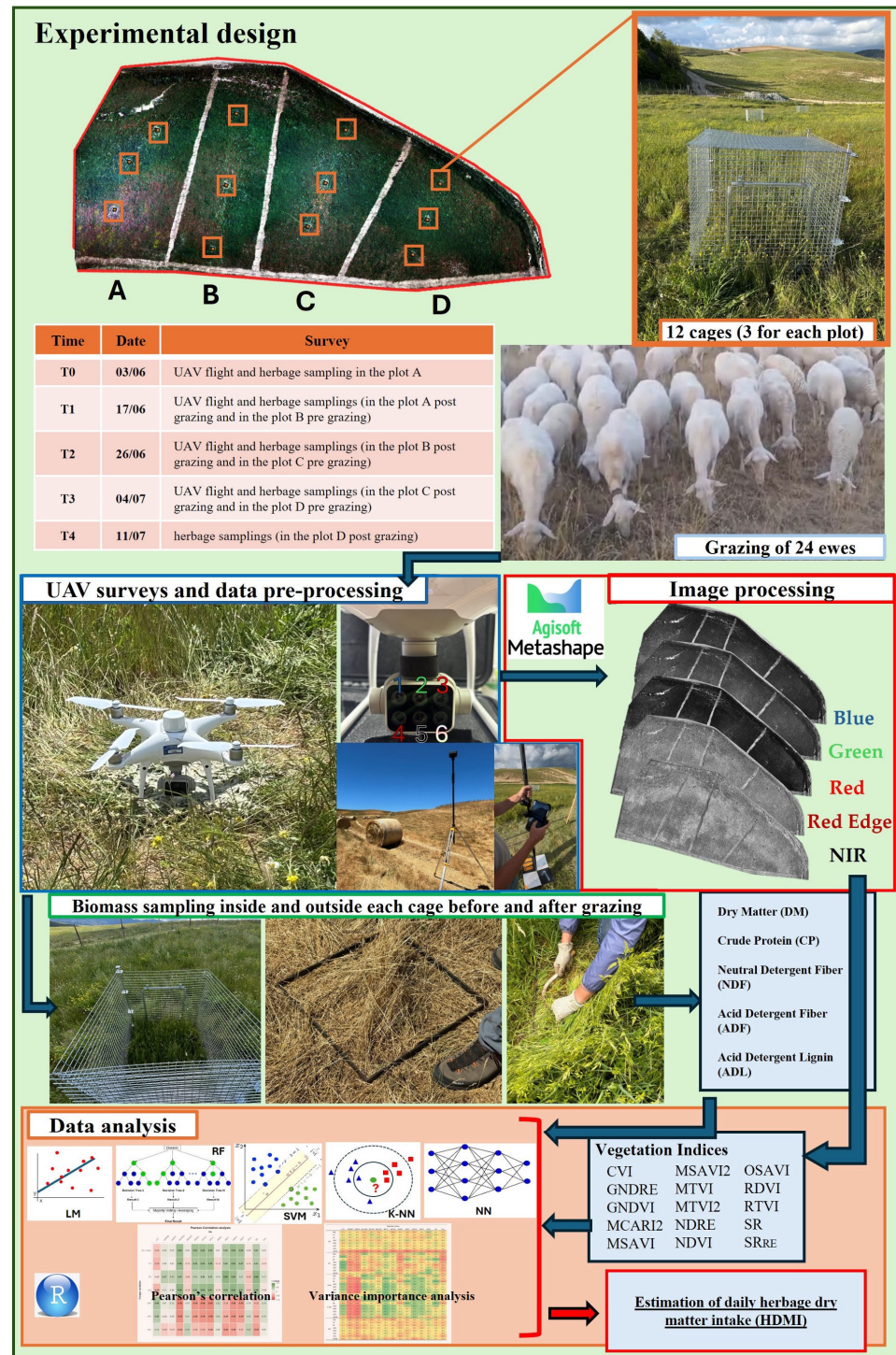


Figure 4. Workflow of the proposed methodology. The first stage illustrates the uncrewed aerial vehicle (UAV) survey and data pre-processing. The second stage presents the image processing procedures and the selected vegetation indices (VIs). The third stage describes the statistical analysis and machine learning (ML) methods.

A reflectance orthomosaic was generated for each spectral band with a spatial resolution of 1 cm. The orthomosaics were calibrated to convert digital numbers into reflectance values using measurements from a field spectroradiometer and a grey polypropylene calibration panel positioned in the field during the UAV flight. Detailed information on the photogrammetric processing can be found in our previous studies [33,39]. The reflectance orthomosaics were then combined to compute a set of VIs as reported in Table 1.

Table 1. List of the vegetation indices (VIs) tested.

Vegetation Index (VI)	Acronym	Formula	Ref
Chlorophyll Vegetation Index	CVI	$\frac{\rho_{NIR}}{\rho_{Green}} \times \frac{\rho_{Red}}{\rho_{Green}}$	[40]
Green Normalised Difference Red Edge	GNDRE	$\frac{\rho_{Red\ Edge} - \rho_{Green}}{\rho_{Red\ Edge} + \rho_{Green}}$	[41]
Green Normalised Difference Vegetation	GNDVI	$\frac{\rho_{NIR} - \rho_{Green}}{\rho_{NIR} + \rho_{Green}}$	[42]
Modified Chlorophyll Absorption Ratio Index	MCARI2	$\frac{1.5 \times [2.5 (\rho_{NIR} - \rho_{Red}) - 1.3 (\rho_{NIR} - \rho_{Green})]}{\sqrt{(2\rho_{NIR} + 1)^2 - (6\rho_{NIR} - 5\rho_{Red}) - 0.5}}$	[43]
Modified Soil Adjusted Vegetation Index	MSAVI	$\frac{NIR - Red}{NIR + Red + L} \times (1 + L)$	[44]
Modified Soil Adjusted Vegetation Index 2	MSAVI2	$\frac{2NIR + 1 - \sqrt{(2NIR + 1)^2 - 8(NIR - Red)}}{2}$	[44]
Modified Triangular Vegetation Index	MTVI	$1.2 \times [1.2 (\rho_{NIR} - \rho_{Green}) - 2.5 (\rho_{Red} - \rho_{Green})]$	[43]
Modified Triangular Vegetation Index 2	MTVI2	$\frac{1.5 \times [1.2 (\rho_{NIR} - \rho_{Green}) - 2.5 (\rho_{Red} - \rho_{Green})]}{\sqrt{(2\rho_{NIR} + 1)^2 - (6\rho_{NIR} - 5\rho_{Red}) - 0.5}}$	[43]
Normalised Difference Red Edge	NDRE	$\frac{\rho_{NIR} - \rho_{Red\ Edge}}{\rho_{NIR} + \rho_{Red\ Edge}}$	[45]
Normalised Difference Vegetation Index	NDVI	$\frac{\rho_{NIR} - \rho_{Red}}{\rho_{NIR} + \rho_{Red}}$	[46]
Optimised Soil Adjusted Vegetation Index	OSAVI	$\frac{1.16 (\rho_{NIR} - \rho_{Red})}{\rho_{NIR} + \rho_{Red} + 0.16}$	[47]
Renormalised Difference Vegetation Index	RDVI	$\frac{\rho_{NIR} - \rho_{Red}}{\sqrt{\rho_{NIR} + \rho_{Red}}}$	[48]
Red Edge Triangulated Vegetation Index	RTVI	$100 [(\rho_{NIR} - \rho_{Red\ Edge}) - 10 (\rho_{NIR} - \rho_{Green})]$	[49]
Simple Ratio	SR	$\frac{\rho_{NIR}}{\rho_{Red}}$	[50]
Simple Ratio Red Edge	SR _{RE}	$\frac{\rho_{NIR}}{\rho_{Red\ Edge}}$	[45]

2.6. Data Management, Statistical and Machine Learning (ML) Approaches

Experimental data were collected and organized in MS Excel™, while predictive approaches were implemented within the RStudio (v.2025.12) environment [51]. To evaluate differences among plots, the forage resource variables were subjected to one-way analysis of variance (ANOVA). When significant differences were detected, multiple comparisons among treatments were performed using Tukey's test ($p < 0.05$). For predictions, the dataset consisted of 36 independent entries that correspond to a 1.0 m² sampling point, with forage traits and VIs expressed as mean values over that area. Pearson's correlations were computed using the cor() function [52], while predictive models were developed and evaluated with the Caret package [53]. Five commonly used models in agricultural research [54,55] were tested: (1) linear model (LM), (2) random forest regression (RF), (3) linear support vector machines (SVM), (4) k-nearest neighbours (k-NN), and (5) neural networks (NN). Forage above-ground plant biomass was estimated by using all VIs retrieved on all measured areas, while HDMI was predicted by using VIs data observed inside (HIC) and outside exclusion cages (HEC). The experimental dataset was split into a training set (70%) and a validation set (30%) to develop and assess model performance. This procedure was repeated 100 times using bootstrap sampling to ensure robust evaluation and to capture the full variability in both training and validation datasets. The ML models were configured with the standard hyperparameters provided by the Caret package, as follows; RF: mtry p/3; ntree 500; node size 5; importance FALSE; SVM: preprocess SCALE; C 1; sigma median of Euclidean distances; k-NN: preprocess SCALE; k 3; distance Euclidean; NN: size 1; decay 0; maxit 100; linout FALSE. For each approach, model performance was evaluated by comparing predictions with the validation dataset using the coefficient of determination (R^2), root mean square error (RMSE), and mean absolute error (MAE), reported at the 50th percentile of the 100 repetitions. The importance of each VIs on the forage variables estimation was assessed using the varImp() function [56].

3. Results and Discussion

3.1. Forage Biomass and Quality Parameters

Data related to the forage production and quality before grazing are reported in Table 2. Experimental data highlight systematic differences in production parameters and chemical composition among the four plots (A–D). Forage biomass, expressed both as DM and FW, was highest in plot A (0.52 and 1.29 kg m⁻², respectively) and showed a progressive reduction down to plot D (0.29 and 0.37 kg m⁻²), indicating a gradual decline in productivity. At the same time, the nutritional fractions of higher feeding value, represented by CP and t EE, decrease along the A–D gradient (CP from 15.83% to 10.00%; EE from 3.66% to 2.46%), while the structural fibre components increase markedly, as evidenced by the rises in NDF, ADF, and ADL (NDF from 48.17% to 63.31%; ADF from 26.93% to 42.58%; ADL from 2.75% to 7.58%). The ash content shows a slight but steady decrease, moving from 8.31% in plot A to 6.16% in plot D.

Table 2. Forage biomass in the four investigated plots before grazing, expressed as dry matter (DM), fresh weight (FW), and its quality parameters: crude protein (CP), ether extract (EE), ash, neutral detergent fibre (NDF), acid detergent fibre (ADF) and acid detergent lignin (ADL). Different letters indicate statistically significant differences ($p < 0.05$).

Plot	DM [kg m ⁻²]	FW [kg m ⁻²]	CP [%]	EE [%]	Ash [%]	NDF [%]	ADF [%]	ADL [%]
A	0.52a ± 0.10	1.29a ± 0.21	15.8a ± 0.6	3.7a ± 0.4	8.3a ± 0.2	48.2d ± 0.7	26.9d ± 0.6	2.7d ± 0.2
B	0.37b ± 0.09	0.54b ± 0.15	15.3a ± 0.3	3.3a ± 0.2	7.1b ± 0.6	50.9c ± 0.7	31.5c ± 0.3	3.7c ± 0.1
C	0.36b ± 0.11	0.47b ± 0.19	12.5b ± 0.3	3.3a ± 0.2	7.0b ± 0.2	58.7b ± 0.4	36.7b ± 0.1	4.4b ± 0.2
D	0.29c ± 0.03	0.37c ± 0.05	10.0c ± 0.2	2.5b ± 0.2	6.2c ± 0.1	63.3a ± 0.2	42.6a ± 0.1	7.6a ± 0.2

The forage DM biomass in the four investigated plots was in line with the productivity observed in other studies conducted in southern European pastures, with values ranging from 0.12 to 0.60 kg m⁻² [57–59]. The protein levels in the fodder, within the range of 8.0 to 19.0%, also correspond to the data observed in other studies [58]. Overall, these results indicate a transition towards progressively more fibrous and less nutrient-rich plant material, with a consequent potential reduction in forage quality and digestibility over the course of the experimental trial. The observed change can be attributed to shifts in environmental conditions during the experimental period, characterized by increased temperature and reduced precipitation, which concurrently induced senescence and decline of white clover, according with botanical analysis (data not showed), the primarily responsible for protein content, and an increase in the fiber content of ryegrass and globally the reduction in quantity and quality of available forage. This scenario typically occurs in rainfed mountain meadows and pastures in southern Italy during the transition from spring to summer, limiting productivity in these areas and posing a challenge for optimal livestock nutrition [60,61]. In addition, in recent years, the effects of global warming and climate change have exacerbated this situation, making it increasingly challenging [62].

Table 3 shows the variations in the production and quality parameters of the forage biomass in the experimental plots (A–D) at the end of the grazing period, separately for the inside (HIC) and outside (HEC) of the exclusion cages. In all plots, the forage biomass, expressed either as DM or FW, was systematically higher in the HIC areas compared to the HEC ones, indicating a clear grazing effect on reducing forage availability. In the same way, some quality parameters such as CP and EE, tend to decrease along the A–D gradient and are generally lower in the EST samples, while the structural fibre fractions (namely, NDF, ADF, and ADL) increase markedly, reaching their highest values in plots C and D. The ash content shows limited variation, with a slight tendency to decrease in the lower-productivity plots.

Table 3. Forage biomass inside (HIC) and outside (HEC) exclusion cages at the end of grazing period in the four investigated plots (A–D), its quality parameters (crude protein—CP, ether extract—EE, ash, neutral detergent fibre—NDF, acid detergent fibre—ADF, and acid detergent lignin—ADL) and herbage dry matter intake (HDMI). Different letters indicate statistically significant differences ($p < 0.05$).

Plot	Sample	DM [kg m ⁻²]	FW [kg m ⁻²]	PG [%]	EE [%]	Ash [%]	NDF [%]	ADF [%]	ADL [%]	HDMI [g m ⁻² d ⁻¹]
A	HIC	0.55a ± 0.05	0.33a ± 0.01	15.1a ± 0.2	3.3a ± 0.1	7.3a ± 0.3	50.7h ± 0.6	31.5g ± 0.1	3.7d ± 0.1	10.61a ± 1.4
	HEC	0.34b ± 0.10	0.18c ± 0.03	13.2b ± 0.1	3.1ab ± 0.1	7.1ab ± 0.5	54.4g ± 0.3	34.8f ± 0.2	4.1c ± 0.2	
B	HIC	0.33b ± 0.02	0.29ab ± 0.01	13.1b ± 0.9	3.4ab ± 0.2	7.0ab ± 0.2	58.7f ± 0.2	36.9e ± 0.2	4.1c ± 0.2	11.78a ± 1.5
	HEC	0.21c ± 0.02	0.18c ± 0.02	11.3c ± 0.2	3.0ab ± 0.1	6.4b ± 0.3	61.7e ± 0.5	39.4d ± 0.1	5.6b ± 0.1	
C	HIC	0.36b ± 0.07	0.32a ± 0.05	10.4c ± 0.2	2.8b ± 0.2	6.4b ± 0.2	63.4d ± 0.3	42.6c ± 0.4	7.3a ± 0.4	8.38b ± 0.5
	HEC	0.30b ± 0.05	0.25b ± 0.05	8.7d ± 0.2	1.9c ± 0.1	6.1c ± 0.1	65.7c ± 0.2	43.9b ± 0.2	7.7a ± 0.2	
D	HIC	0.29b ± 0.04	0.24b ± 0.04	7.6e ± 0.1	1.9c ± 0.4	6.1c ± 0.2	69.0b ± 0.4	46.1a ± 0.1	7.3a ± 0.1	6.25c ± 0.5
	HEC	0.24b ± 0.04	0.20c ± 0.04	6.4f ± 0.1	2.0c ± 0.1	6.0c ± 0.2	70.2a ± 0.1	46.4a ± 0.2	7.4a ± 0.2	

Data related to the HDMI for all four investigated plots are reported in Table 3 and ranged from 6.25 to 10.61 g m⁻² d⁻¹, in accordance with what has been observed by several studies involving dairy sheep [63–65]. The recorded data, compared with those found in the literature, are representative of an extensive, low-productivity forage system where intake by the ewes was moderate. The HDMI values show a progressive decrease from plot A to plot D, consistent with the decline in productivity and the increase in fibrous fractions. Overall, the results highlight a progressive deterioration in forage quality and digestibility associated [66,67] with increased fibre content and a reduction in the animals’ daily dry matter intake during the trial, for the same reasons stated above regarding forage production data prior to grazing.

3.2. Pearson’s Correlation Analysis Between VIs, Forage Biomass and Its Quality Parameters

Results of Pearson’s correlation analysis between VIs, forage biomass and its quality parameters are reported in the following Figure 5.

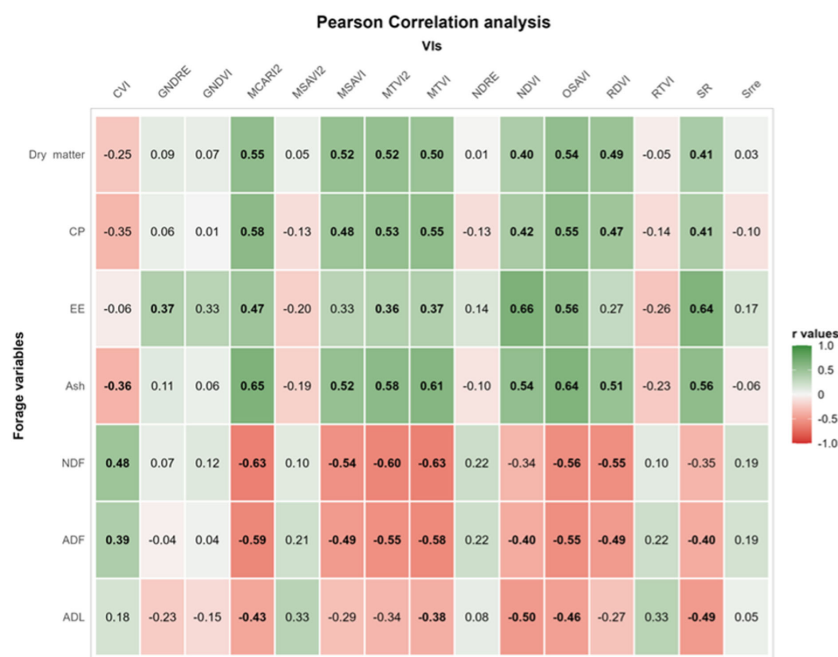


Figure 5. Results of Pearson’s correlations analysis between VIs, forage biomass dry matter and its quality parameters (crude protein—CP, ether extract—EE, ash, neutral detergent fibre—NDF, acid detergent fibre—ADF and acid detergent lignin—ADL). Correlation values (r) are reported inside the cell that is painted by a different colour, ranging from green (positive correlation) to red (negative correlation). Values of r in bold indicate statistically significant correlations ($p < 0.05$).

In general, moderately significant correlations were retrieved, with the highest r values observed equal to 0.66, with several VIs. With regard to dry matter, 8 of 15 VIs investigated showed significant and positive correlation with this variable, with r values ranging from 0.41 of SR to 0.55 of MCARI2. The CP concentration showed significant correlation with the same VIs, with the highest r values observed for MCARI2 equal to 0.58. For the ether extract, relevant correlations were observed with NDVI (0.66), OSAVI (0.56) and SR (0.64), while for ash, many more significant relationships were observed, such as those with MCARI2 (0.65), OSAVI (0.64), MTVI (0.61) and MTVI2 (0.58). With regard to the fibre fractions content, generally, negative correlations were observed with most spectral indices, the strongest of which were those with MCARI2 (−0.63), MTVI (−0.63), MTVI2 (−0.60) and OSAVI (−0.56).

A reliable estimation of forage availability and quality in grassland is indispensable to properly support livestock farming. Considering the field experimental data, which highlighted a rapid temporal decay and variability in the quantity and quality of available forage, driven by weather and climatic conditions, an accurate estimate of forage resources in Mediterranean agro-pastoral systems becomes crucial to prevent overgrazing and to ensure the best possible nutrition for livestock. This, in turn, safeguards animal welfare and productivity, further supported by an improved and precise formulation of dietary supplementation [68]. Conventional approaches based on field sampling and laboratory analyses are destructive, labor-intensive, and expensive, as they require a large number of samples to reliably characterize a field. With the aim of overcoming the limitations of traditional approaches, it is essential to implement new remote sensing technologies, such as the use of UAVs equipped with sensors capable of monitoring the spectral response of crop fields. Therefore, it is important to understand which VI yield the best performance, both in correlation analyses and when used in predictive models, for each specific forage system context. This necessity arises from the fact that differences among various forage agroecosystems are highly pronounced due to spatial diversity in species composition and distribution [69]. Furthermore, these species are often not cultivated in pure stands but in associations or mixtures with other species; indeed, polycultures and mixed-species stands are common [70].

Among the studied VIs, the best performances for almost all forage variables were achieved by MCARI2, MTVI2, MTVI, MSAVI and OSAVI; it is noteworthy that the first three indices incorporate the Green band in their equation, whereas all, with the exception of MTVI, are normalized for NIR and Red band. In particular, our findings, with respect to MCARI2 and MTVI performances, confirm the importance of the Red, Green and NIR bands, as well as normalisation for the red and NIR bands, to achieve a good remote sensing of heterogeneous cover such as that of pastures consisting of soil and plants of different species. Thus, our results agree with those of Togeiro de Alckmin et al. [71], who observed good performance by the same VIs in an ordinary linear regression for perennial ryegrass biomass prediction, Sangjan et al. [72] and Fern et al. [73], where MCARI2 and OSAVI indices were shown to be effective for differentiating between the various grazing treatments, and Haboudane et al. [43], who find that MCARI2 and MTVI2 are the best predictors of green LAI, particularly important in heterogeneous cover. With regard to the CP estimation, our study confirms the importance of NIR for the estimation of this variable in plants according to Wijesingha et al. [74].

Generally, the best performing models showed opposite correlation between DM, CP, EE, ash and fibre fractions percentages. This can be attributed to the progression of the senescence process in part of the pasture's plant biomass. As sampling progressed over time, this led to a decrease in DM and CP content (with EE and ash content being closely related to these parameters) and, consequently, an increase in fibre content, particularly

NDF and ADL. Specifically, the loss of white clover, which was depleted after the first two sampling dates, as described above, contributed significantly to the change in protein and fibre content.

NDVI and GNDVI are typically correlated with photosynthetically [75] active radiation and are often reported as two indices capable of interpreting the vigour of plants [76–78]. However, in our study, we did not observe a significant correlation between the values of these two VIs and quantitative/qualitative forage parameters, except for ash and EE for NDVI. Discarding the possibility that this index could have reached saturation, often observed in other studies (e.g., [79,80]), our findings confirm how important it is in this context to use indices that include the Green band and are optimised to correct for the influence of the brightness of the underlying ground, compared to other higher-performing indices. In addition, as postulated by Luns Hatum de Almeida et al. [81], Serrano et al. [82] and Barnes et al. [83], the progression of flowering and ageing processes of grasses had an effect on the NDVI values, with an increase in Red reflectance and a decrease in NIR reflectance, reducing the predictive capabilities of this index, according to Serrano et al. [82] and Togeiro de Alckmin et al. [71]. For the same reason, the prediction capabilities of VIs, which include the Red Edge band, were unsatisfactory, despite other authors’ claims [84,85].

3.3. Modelling Approaches for Forage Biomass and Quality Estimation

In the following Tables 4–6, the results of the five different model approaches tested are presented, observed in 50% of the 100 repetitions. With regard to the estimation of DM, the best predictions were achieved by SVM and NN that reached R² values of 0.63 with a RMSE of 0.07 and 0.08 kg m⁻², respectively. For the estimation of HDMI the tested model performed better with R² values observed, with the exception of LM, higher than 0.80; in particular, NN approached showed R² equal to 0.91 and a RMSE of 1.29 g m⁻² d⁻¹ while R² of 0.89 and RMSE of 1.32 g m⁻² d⁻¹ were those of RF (Table 4).

Table 4. Models (linear model—LM, random forest regression—RF, linear support vector machines—SVM, k-nearest neighbors—k-NN, and neural networks—NN) validation performance-related data for forage dry matter (DM) and herbage dry matter intake (HDMI) estimation: coefficient of determination (R²), root mean square error (RMSE) and mean absolute error (MAE).

		DM			HDMI		
		R ²	RMSE	MAE	R ²	RMSE	MAE
Models	LM	0.44	0.11	0.13	0.63	2.23	2.34
	RF	0.51	0.07	0.09	0.89	1.32	1.42
	SVM	0.63	0.06	0.08	0.81	1.54	1.76
	k-NN	0.44	0.12	0.15	0.87	1.47	1.7
	NN	0.63	0.08	0.09	0.91	1.29	1.54

Table 5. Models (linear model—LM, random forest regression—RF, linear support vector machines—SVM, k-nearest neighbors—k-NN, and neural networks—NN) validation performance-related data for crude protein (CP) ether extract (EE) and ash estimation: coefficient of determination (R²), root mean square error (RMSE) and mean absolute error (MAE).

		CP			EE			Ash		
		R ²	RMSE	MAE	R ²	RMSE	MAE	R ²	RMSE	MAE
Models	LM	0.35	2.69	3.2	0.42	0.49	0.57	0.62	0.48	0.59
	RF	0.54	1.30	1.67	0.57	0.29	0.37	0.72	0.33	0.43
	SVM	0.63	1.33	1.66	0.65	0.25	0.32	0.84	0.28	0.35
	k-NN	0.47	1.46	1.84	0.57	0.32	0.38	0.68	0.38	0.45
	NN	0.47	1.61	2.00	0.63	0.31	0.36	0.67	0.37	0.47

Table 6. Models (linear model—LM, random forest regression—RF, linear support vector machines—SVM, k-nearest neighbors—k-NN, and neural networks—NN) validation performance-related data neutral detergent fibre (NDF), acid detergent fibre (ADF) and acid detergent lignin (ADL): coefficient of determination (R^2), root mean square error (RMSE) and mean absolute error (MAE).

		NDF			ADF			ADL		
		R^2	RMSE	MAE	R^2	RMSE	MAE	R^2	RMSE	MAE
Models	LM	0.42	5.99	7.15	0.47	4.45	5.38	0.48	1.84	2.25
	RF	0.56	3.17	4.12	0.57	2.78	3.81	0.59	1.00	1.2
	SVM	0.70	2.99	3.65	0.73	2.64	3.16	0.68	0.94	1.16
	k-NN	0.58	3.63	4.34	0.56	3.29	4.05	0.48	1.23	1.44
	NN	0.38	4.06	5.02	0.44	3.60	4.37	0.44	1.08	1.48

With regard to the estimation of quality parameters CP, EE and ash, among the investigated models, SVM showed the best performance with R^2 of 0.63, 0.65 and 0.84, followed by RF with R^2 of 0.54, 0.57, and 0.72, respectively (Table 5).

Even for the estimation of plant constituents' fibre, NDF, ADF and ADL, the model that provided the best estimates was SVM, highlighting values of R^2 equal to, respectively, 0.70, 0.73 and 0.68 (Table 6). The other prediction models compared to SVM, with the exception of ash concentration, have recorded poor performance on the estimation of forage quality variables.

The predictive performance of the various ML models consistently surpassed that of Pearson's correlations between VIs and pasture biomass. This aligns with existing literature, which attributes the reliability of ML for yield prediction to its capacity to model non-linear interactions and mitigate the influence of spurious data [85–87]. Specifically, ML models produced R^2 values consistently above those of Pearson correlation. Moreover, the predictive robustness of the ML approach is further emphasized by the fact that it was validated using a held-out dataset, a more rigorous test than the single-dataset evaluation applied to the correlation analysis.

Overall, among all forage variables, SVM, NN and RF showed the best performances among the tested models. In particular, SVM was the best method to predict almost every individual variable, while NN and RF showed slightly better performance for HDMI estimation. The results demonstrate that all three modelling strategies could extract meaningful patterns from complex spectral data. These results further support the robustness of ML approaches in modelling crop-related variables through their ability to capture complex and non-linear patterns that characterise the raw data from UAV-based multispectral survey, as also reported by previous studies [86–88]. Notably, unlike Pearson's correlation analysis, which was conducted on the full dataset, the ML models were evaluated using separate training and validation subsets, thereby providing stronger evidence of their predictive capability. Despite challenges related to noise, predictor interdependence, and model overfitting, each method effectively processed multiple input variables and produced accurate predictions of forage biomass and quality traits, typically affected by considerable variability in the field. Therefore, these findings may promote the rapid and practical application of the derived VIs values for forage resources estimation in the pasture, supporting livestock farmers.

The SVMs are supervised learning models that aim to identify an optimal decision boundary, known as a hyperplane, that best fits the data. The SVMs focus on maximizing the margin between data points and the hyperplane while minimizing prediction errors. The position and orientation of this boundary are determined by a subset of critical training points, referred to as support vectors, which have the greatest influence on the model [88,89]. The NNs are computational models developed to capture complex relationships in data and perform tasks such as classification and regression. Inspired by the structure of the

human brain, they consist of interconnected processing units, the neurons, arranged in layers that convert inputs into meaningful outputs through iterative training [90]. RF is an ensemble learning technique that aggregates the predictions of multiple decision trees to improve overall accuracy and robustness. By constructing each tree on random bootstrap sampled subsets of the data and predictors (called bagging), the method reduces variance and mitigates overfitting, resulting in more stable and reliable predictions for both classification and regression tasks [91]. Results consistent with those we found regarding the best performance achieved by these three models in estimating forage resources in pastures were presented in studies by Adar et al. [92] (SVM), Belgiu and Dra [93] (RF), Alvarez-Mendoza et al. [94] (RF), Wang et al. [95] (RF), Pullanagari et al. [96] (RF), Mas and Flores [97] (NN), and Mutanga et al. [98] (NN). With specific reference to the CP variable, good performance by SVM was also observed by Wijesingha et al. [74].

In estimating the HDMI, the use of spectral information from both outside and inside the grazing enclosures cages resulted in superior estimation performance for this variable compared to that achieved for forage biomass estimation alone. This underscores the importance of establishing ungrazed reference areas, or check plots, in the field for the purpose of estimating this specific parameter. This approach mirrors the methodology used in estimating the nitrogen requirements of herbaceous crops, where check plots with varying nutrient levels are established to guide and improve the accuracy of crop demand predictions (e.g., the NNI concept applied to remote sensing as presented in Liu et al. [99]). Therefore, the present study demonstrates the suitability of integrating UAV multispectral imagery with ML approaches, especially NN and RF models, to assess pasture depletion for improved grazing animal management. In particular, the results showed that these two approaches are more robust and better able to handle the larger amount of data, most likely effects of multi-collinearity, used for HDMI estimation than the SVM approach, as observed by Yue et al. [100]. Our findings are in agreement with those of Álvarez-Hess et al. [101], who reported positive results from the use of UAV imagery and modelling techniques for estimating pasture consumption; however, unlike their study, we relied on a less advanced UAV platform using multispectral imagery.

The results of the relative importance analysis of VIs used in the tested model are reported in Figure 6. In general, variable importance analysis highlighted differences between models and, for each, between VIs. For LM and NN, the relative importance was generally similar among VIs and only in some cases has exceeded the value of 60, like RTVI for DM estimation, CVI and NDVI for ash estimation, and MSAVI2 and RTVI for EE estimation. For the other models (RF, SVM, k-NN), the difference among VIs' importance was greater, with some indices showing greater importance and significance than others. In addition, a selective importance of the different VIs was observed among the tested models in the estimation of DM/HDMI and forage quality parameters. In those three models, greater importance for the estimation of DM had MCARI2, MSAVI, MTVI, MTVI2, NDVI, OSAVI, RDVI (only for RF), and SR, while for the estimation of HDMI, the most relevant VIs were MSAVI, MTVI, MTVI2, NDVI, OSAVI, RDVI and SR. The estimation of forage qualitative variables highlighted the greater importance of CVI, MCARI2, MSAVI, MTVI, MTVI2, OSAVI, RDVI and RTVI.

		Vegetation indices														
		CVI	GNDRE	GNDVI	MCARI2	MSAVI	MSAVI2	MTVI	MTVI2	NDRE	NDVI	OSAVI	RDVI	RTVI	SR	Srre
LM	DM	37.1	42.2	42.0	33.9	34.7	34.4	45.1	29.8	39.3	34.8	32.1	44.9	66.9	43.1	37.5
	CP	49.5	52.3	48.7	36.1	59.9	36.1	45.7	39.6	43.9	39.9	38.5	36.3	31.2	56.4	37.0
	EE	47.4	52.7	49.2	34.0	53.5	60.7	34.0	39.5	48.7	35.3	32.6	31.8	66.2	45.1	39.2
	ASH	60.1	36.4	35.6	39.2	33.9	31.2	44.1	45.5	42.7	60.4	38.4	36.1	45.8	38.0	49.6
	NDF	34.8	56.3	54.7	40.1	53.4	35.1	56.6	36.7	48.7	35.5	43.1	43.1	35.9	54.6	43.3
	ADF	40.1	50.0	48.2	42.2	57.0	38.9	55.4	32.3	46.0	36.5	39.1	43.9	41.4	53.5	37.3
	ADL	43.3	43.8	43.7	39.6	43.9	43.6	56.7	38.0	46.2	42.1	38.1	42.2	52.7	47.3	44.9
	HDMI	22.1	15.8	10.8	5.5	18.4	17.0	22.1	7.5	17.1	5.1	17.1	22.1	12.5	13.5	18.5
RF	DM	29.8	29.2	25.0	80.8	53.0	35.0	76.1	57.9	22.3	57.9	63.7	77.6	36.6	61.3	21.5
	CP	91.2	25.9	21.1	47.6	34.8	40.6	69.2	49.6	16.5	29.4	35.1	49.2	52.3	34.2	15.4
	EE	46.6	24.7	22.0	39.5	30.9	56.7	48.8	42.6	12.9	84.5	56.1	33.9	70.5	91.2	9.5
	ASH	91.9	13.5	22.2	56.7	28.5	34.5	57.4	55.0	21.8	51.9	50.3	32.1	44.5	56.7	21.1
	NDF	94.9	15.8	12.9	53.5	33.4	27.0	66.4	51.8	29.1	19.3	29.0	43.6	35.7	22.4	25.2
	ADF	93.0	21.9	17.0	44.8	32.4	37.8	63.5	48.1	24.5	27.9	33.5	46.6	59.4	31.1	24.8
	ADL	78.7	18.5	17.6	29.4	23.5	62.9	46.2	33.6	21.1	53.1	36.2	37.6	80.2	60.0	22.1
	HDMI	40.1	44.7	41.9	36.2	49.4	75.7	62.3	58.3	29.9	48.0	29.7	72.8	82.2	47.5	32.1
SVM	DM	32.8	28.8	46.6	89.7	70.2	25.3	59.1	68.3	37.9	77.5	73.7	51.1	34.0	76.6	32.7
	CP	68.7	11.4	7.4	77.6	72.1	45.5	93.9	76.9	36.1	54.1	82.4	83.9	51.3	56.1	35.4
	EE	37.2	17.3	13.9	45.6	45.1	36.5	73.0	48.1	21.2	91.7	78.3	78.2	52.5	95.2	20.8
	ASH	83.1	11.7	5.0	78.6	60.0	49.9	90.7	73.6	53.4	67.6	84.8	73.5	58.4	69.0	51.6
	NDF	76.7	10.8	2.6	82.1	71.7	44.1	94.4	78.7	45.6	37.7	76.2	78.9	49.6	38.7	44.1
	ADF	77.9	10.0	4.0	77.6	68.9	54.0	91.4	77.0	54.2	50.8	80.1	79.3	63.9	53.3	52.5
	ADL	63.3	9.0	2.9	48.1	51.2	69.5	89.9	64.9	46.7	67.2	64.3	79.8	68.8	68.1	46.2
	HDMI	33.1	28.8	46.6	49.7	72.1	49.5	94.4	78.7	44.2	71.7	74.8	83.9	48.8	85.2	42.5
k-NN	DM	32.7	36.8	51.4	89.1	69.9	26.5	56.9	69.6	31.5	75.5	75.2	50.5	27.8	73.1	26.7
	CP	63.4	9.6	4.7	77.7	72.4	48.6	95.4	78.4	37.8	55.5	80.8	83.5	50.6	60.0	36.8
	EE	29.9	15.0	14.4	45.2	45.3	35.4	70.1	47.5	21.2	89.8	78.3	73.7	48.4	93.7	20.9
	ASH	84.3	7.7	5.3	81.4	65.0	46.9	91.7	77.6	50.2	71.2	86.2	76.2	60.5	74.0	48.9
	NDF	78.9	11.0	4.9	81.5	73.4	45.0	92.7	79.3	48.5	39.8	77.8	79.7	52.8	40.7	47.5
	ADF	77.7	11.2	4.4	76.0	68.6	55.0	90.1	76.6	56.1	48.1	79.3	77.2	66.5	49.4	54.2
	ADL	75.9	8.6	4.4	66.1	64.8	52.6	90.4	66.3	61.0	45.5	77.1	73.8	61.5	47.1	52.2
	HDMI	33.3	14.3	12.8	73.9	65.6	24.3	73.9	70.7	33.8	60.8	79.2	53.5	32.6	62.6	31.0
NN	DM	48.9	23.4	23.5	28.4	29.9	39.0	29.3	19.2	42.0	34.4	36.2	53.7	64.3	33.8	39.1
	CP	47.0	35.3	30.4	42.3	34.1	32.1	44.4	40.7	28.1	34.1	34.7	34.9	49.0	35.2	32.1
	EE	36.3	24.2	24.7	30.4	41.4	44.9	39.4	34.0	30.4	34.6	29.5	33.3	57.3	33.6	34.2
	ASH	45.1	32.4	24.2	33.6	36.7	42.0	42.0	40.1	32.0	47.2	38.5	32.0	45.3	49.0	39.0
	NDF	50.4	40.4	32.4	42.3	43.5	41.1	50.2	42.3	45.0	31.7	36.4	48.5	41.2	44.8	46.2
	ADF	43.4	35.4	28.1	46.0	41.3	43.1	53.9	42.0	31.7	33.2	45.9	40.6	41.9	43.7	38.0
	ADL	33.8	27.9	22.0	27.0	32.2	44.6	47.2	43.2	26.6	36.4	43.3	42.3	48.8	40.9	26.7
	HDMI	33.0	37.3	35.7	22.0	30.3	57.6	27.1	26.5	36.6	37.0	22.1	31.5	52.7	41.1	37.5

Figure 6. Results of variance importance analysis performed on 15 different vegetation indices used in five different predictive models (linear model—LM, random forest regression—RF, linear support vector machines—SVM, k-nearest neighbours—k-NN, and neural networks—NN) for the estimation of forage dry matter (DM) and herbage dry matter intake (HDMI), crude protein (CP) ether extract (EE) ash, neutral detergent fibre (NDF), acid detergent fibre (ADF) and acid detergent lignin (ADL).

4. Conclusions

This study demonstrated the effectiveness of integrating field measurements, UAV-based multispectral remote sensing, and ML techniques to assess pasture productivity and quality, as well as animal intake dynamics in Mediterranean extensive grazing systems. The combined approach enabled the characterisation of spatial and temporal variability in pasture resources, highlighting a progressive seasonal decline in forage biomass and nutritional quality across the investigated plots. This decline was associated with increasing fibre fractions and decreasing crude protein and ether extract contents, primarily driven by seasonal climatic conditions characterised by increasing temperatures and reduced precipitation. These conditions accelerated plant senescence and reduced the contribution of high-nutritional-value species, such as white clover, with direct implications for grazing system productivity and stability.

Correlation analysis confirmed that several vegetation indices were moderately associated with forage biomass and quality parameters, particularly indices integrating green reflectance and normalized red and near-infrared bands. Among the evaluated indices, MCARI2, MTVI2, MTVI, MSAVI, and OSAVI consistently showed the highest predictive performance across multiple forage variables, demonstrating strong suitability for mon-

itoring heterogeneous mixed-species grasslands where soil background variability and botanical composition complexity represent key limiting factors for traditional remote sensing approaches.

Machine learning approaches outperformed conventional correlative methods, confirming their ability to capture nonlinear relationships between spectral data and pasture biophysical variables. Support Vector Machines achieved the highest overall predictive accuracy for forage biomass and quality parameters, while Neural Networks and Random Forest models showed slightly superior performance for herbage dry matter intake estimation. Importantly, the integration of spectral information derived from grazed and ungrazed reference areas significantly improved intake prediction accuracy, highlighting the relevance of exclusion cages or control plots for operational grazing monitoring frameworks.

The results confirm the strong potential of UAV multispectral data combined with advanced modelling approaches to support precision grazing management. The integration of forage availability, nutritional quality indicators, and intake estimation into digital data management systems provides robust decision-support tools capable of improving grazing efficiency, preventing overgrazing, and reducing nutritional stress in grazing livestock. From a land system perspective, this contributes to improving resource use efficiency, maintaining vegetation functionality, and supporting the long-term sustainability of low-input pastoral systems.

From a management and environmental perspective, the proposed approach provides a scalable and transferable framework for Mediterranean agro-pastoral landscapes, where forage resources are highly heterogeneous and strongly influenced by climatic variability. The integration of remote sensing, machine learning, and animal response data represents a key step toward data-driven pasture management, contributing to the maintenance of ecosystem services such as soil protection, carbon storage, and biodiversity conservation. This approach supports the transition toward climate-resilient grazing systems and sustainable land use strategies under increasing climate pressure.

Future research should focus on scaling UAV monitoring to larger spatial extents and diverse botanical compositions, integrating additional environmental variables, and incorporating emerging sensor technologies to improve model robustness and generalization capacity. Further efforts should also address the development of integrated indicators linking pasture productivity, soil health, biodiversity, and carbon sequestration potential. These advancements will support the implementation of multifunctional, climate-resilient, and environmentally sustainable grazing systems within Mediterranean and other climate-vulnerable pastoral regions.

Author Contributions: Conceptualization, P.C., S.P. and G.B.; methodology, P.C., S.P., G.M. and G.B.; software, S.P. and G.B.; validation, G.M. and G.B.; formal analysis, P.C., S.P., C.C., P.D.C., G.M. and G.B.; investigation, P.C., S.P., C.C., P.D.C., G.M. and G.B.; resources, P.C., S.P. and G.B.; data curation, P.C., S.P., C.C., G.M., P.D.C. and G.B.; writing—original draft preparation, P.C., S.P., G.M. and G.B.; writing—review and editing, P.C., S.P., G.M., C.C., P.D.C., E.L.P., A.B., A.D.T., R.P. and G.B.; visualization, G.M. and G.B.; supervision, P.C., S.P. and G.B.; project administration, P.C.; funding acquisition, P.C. All authors have read and agreed to the published version of the manuscript.

Funding: This work and the APC were funded by the Next Generation EU—Italian NRRP, Mission 4, Component 2, Investment 1.5, call for the creation and strengthening of ‘Innovation Ecosystems’, building ‘Territorial R&D Leaders’ (Directorial Decree n. 2021/3277)—“Project Tech4You—Technologies for climate change adaptation and quality of life improvement”, identification code ECS00000009, Unique Project Code C33C22000290006. This work reflects only the authors’ views and opinions; neither the Ministry for University and Research nor the European Commission can be considered responsible for them.

Data Availability Statement: The raw data supporting the conclusions of this article will be made available by the authors on request.

Acknowledgments: The authors acknowledge that the methodology and results presented in this study were developed within the framework of the NRRP Project “Tech4You”, Spoke 3, Goal 3.1, Pilot Project (PP) 3.1.1, Action 3.1.1.7 “Precision Small Ruminant Farming”. The authors also acknowledge the scientific supervision of Pasquale Caparra, who was responsible for Action 3.1.1.7 within this project. The authors thank the owners of the pilot livestock farm “Fattoria Biò”, Francesco, Mario, Saverio, and Luigi Grillo, for their support and collaboration, Giovanni Lumia and Tommaso Bianco for their technical contributions.

Conflicts of Interest: The authors declare no conflicts of interest.

References

1. Suttie, J.M.; Reynolds, S.G.; Batello, C. *Grasslands of the World*; FAO Plant Production and Protection Series No. 34; Food and Agriculture Organization of the United Nations: Rome, Italy, 2005; ISBN: 92-5-105337-5, ISBN-13: 978-92-5-105337-9.
2. Lemaire, G.; Hodgson, J.; Chabbi, A. (Eds.) *Grassland Productivity and Ecosystem Services*; CABI Publishing: Wallingford, UK, 2011; ISBN 978-1-84593-809-3. [[CrossRef](#)]
3. Intergovernmental Panel on Climate Change (IPCC). *Climate Change and Land: An IPCC Special Report on Climate Change, Desertification, Land Degradation, Sustainable Land Management, Food Security, and Greenhouse Gas Fluxes in Terrestrial Ecosystems*; Cambridge University Press: Cambridge, UK, 2019; Volume 152, p. 7. ISBN 978 92 9169. [[CrossRef](#)]
4. Porqueddu, C.; Ates, S.; Louhaichi, M.; Kyriazopoulos, A.P.; Moreno Marcos, G.; del Pozo, A.; Ovalle, C.; Ewing, M.A.; Nichols, P.G.H. Grasslands in ‘Old World’ and ‘New World’ Mediterranean Climate Zones: Past Trends, Current Status and Future Research Priorities. *Grass Forage Sci.* **2016**, *71*, 1–35. [[CrossRef](#)]
5. Pergola, M.; De Falco, E.; Cerrato, M. Grassland Ecosystem Services: Their Economic Evaluation through a Systematic Review. *Land* **2024**, *13*, 1143. [[CrossRef](#)]
6. Elliott, J.; Tindale, S.; Outhwaite, S.; Nicholson, F.; Newell Price, P.; Sari, N.H.; Hunter, E.; Sánchez Zamora, P.; Jin, S.; Gallardo Cobos, R.; et al. European Permanent Grasslands: A Systematic Review of Economic Drivers of Change, Including a Detailed Analysis of the Czech Republic, Spain, Sweden, and UK. *Land* **2024**, *13*, 116. [[CrossRef](#)]
7. Patera, V.; Di Fazio, S.; Messina, G.; Praticò, S. The Application of Remote Sensing Technologies in Pastures Monitoring: A Review for the Mediterranean Region. *Sustainability* **2026**, *18*, 1642. [[CrossRef](#)]
8. Martins-Noguerol, R.; Moreno-Pérez, A.J.; Pedroche, J.; Gallego-Tévar, B.; Cambrollé, J.; Matías, L.; Fernández-Rebollo, P.; Martínez-Force, E.; Pérez-Ramos, I.M. Climate Change Alters Pasture Productivity and Quality: Impact on Fatty Acids and Amino Acids in Mediterranean Silvopastoral Ecosystems. *Agric. Ecosyst. Environ.* **2023**, *358*, 108703. [[CrossRef](#)]
9. Plieninger, T.; Draux, H.; Fagerholm, N.; Bieling, C.; Bürgi, M.; Kizos, T.; Kuemmerle, T.; Primdahl, J.; Verburg, P.H. The Driving Forces of Landscape Change in Europe: A Systematic Review of the Evidence. *Land Use Policy* **2016**, *57*, 204–214. [[CrossRef](#)]
10. Aquilani, C.; Confessore, A.; Bozzi, R.; Sirtori, F.; Pugliese, C. Review: Precision Livestock Farming Technologies in Pasture-Based Livestock Systems. *Animal* **2021**, *16*, 100429. [[CrossRef](#)]
11. Paolino, R.; Di Trana, A.; Coppola, A.; Sabia, E.; Riviezzi, A.M.; Vignozzi, L.; Claps, S.; Caparra, P.; Pacelli, C.; Braghieri, A. May the Extensive Farming System of Small Ruminants Be Smart? *Agriculture* **2025**, *15*, 929. [[CrossRef](#)]
12. Hodgson, J. *Grazing Management: Science into Practice*; Longman Scientific and Technical: Harlow, UK, 1990; p. 203. ISBN 978 0582450103/978 0470216446.
13. Susruthan, V.; Donaghy, D.J.; Kenyon, P.R.; Sneddon, N.W.; Cartmill, A.D. Measuring Herbage Mass: A Review. *Agronomy* **2025**, *15*, 2264. [[CrossRef](#)]
14. Wang, Z.; Ma, Y.; Zhang, Y.; Shang, J. Review of Remote Sensing Applications in Grassland Monitoring. *Remote Sens.* **2022**, *14*, 2903. [[CrossRef](#)]
15. Michez, A.; Lejeune, P.; Bauwens, S.; Herinaina, A.A.L.; Blaise, Y.; Castro-Muñoz, E.; Lebeau, F.; Bindelle, J. Mapping and Monitoring of Biomass and Grazing in Pasture with an Unmanned Aerial System. *Remote Sens.* **2019**, *11*, 473. [[CrossRef](#)]
16. Lussem, U.; Bolten, A.; Kleppert, I.; Jasper, J.; Gnyp, M.L.; Schellberg, J.; Bareth, G. Herbage Mass, N Concentration, and N Uptake of Temperate Grasslands Estimated from UAV-Based Image Data Using Machine Learning. *Remote Sens.* **2022**, *14*, 3066. [[CrossRef](#)]
17. Viljanen, N.; Honkavaara, E.; Näsi, R.; Hakala, T.; Niemeläinen, O.; Kaivosoja, J. A Novel Machine Learning Method for Estimating Biomass of Grass Swards Using a Photogrammetric Canopy Height Model, Images and Vegetation Indices Captured by a Drone. *Agriculture* **2018**, *8*, 70. [[CrossRef](#)]

18. Paolino, R.; Sabia, E.; Braghieri, A.; Riviezzzi, A.M.; Vignozzi, L.; Claps, S.; Baldassarre, D.; Pacelli, C.; Caparra, P.; Di Trana, A. Methodological Approaches for Estimating the Biomass of Natural Pastures in the Lucanian Hills Using UAV Remote Sensing. In *Proceedings of I4SDG Workshop 2025—IFTToMM for Sustainable Development Goals. I4SDG 2025*; Carbone, G., Quaglia, G., Eds.; Mechanisms and Machine Science; Springer: Cham, Switzerland, 2025; Volume 179. [[CrossRef](#)]
19. Ali, A.; Kaul, H.-P. Monitoring Yield and Quality of Forages and Grassland in the View of Precision Agriculture Applications—A Review. *Remote Sens.* **2025**, *17*, 279. [[CrossRef](#)]
20. Mutanga, O.; Skidmore, A.K. Narrow Band Vegetation Indices Overcome the Saturation Problem in Biomass Estimation. *Int. J. Remote Sens.* **2004**, *25*, 3999–4014. [[CrossRef](#)]
21. Adar, S.; Sternberg, M.; Argaman, E.; Henkin, Z.; Dovrat, G.; Zaady, E.; Paz-Kagan, T. Testing a Novel Pasture Quality Index Using Remote Sensing Tools in Semiarid and Mediterranean Grasslands. *Agric. Ecosyst. Environ.* **2023**, *357*, 108674. [[CrossRef](#)]
22. Maresma, Á.; Ariza, M.; Martínez, E.; Lloveras, J.; Martínez-Casasnovas, J.A. Analysis of Vegetation Indices to Determine Nitrogen Application and Yield Prediction in Maize (*Zea mays* L.) from a Standard UAV Service. *Remote Sens.* **2016**, *8*, 973. [[CrossRef](#)]
23. Liakos, K.G.; Busato, P.; Moshou, D.; Pearson, S.; Bochtis, D. Machine Learning in Agriculture: A Review. *Sensors* **2018**, *18*, 2674. [[CrossRef](#)]
24. Pullanagari, R.R.; Yule, I.J.; Tuohy, M.P.; Hedley, M.J.; Dynes, R.A.; King, W.M. In-field hyperspectral proximal sensing for estimating quality parameters of mixed pastures. *Precis. Agric.* **2012**, *13*, 351–369. [[CrossRef](#)]
25. Kamilaris, A.; Prenafeta-Boldú, F.X. Deep Learning in Agriculture: A Survey. *Comput. Electron. Agric.* **2018**, *147*, 70–90. [[CrossRef](#)]
26. Grüner, E.; Astor, T.; Wachendorf, M. Biomass Prediction of Heterogeneous Temperate Grasslands Using an SfM Approach Based on UAV Imaging. *Agronomy* **2019**, *9*, 54. [[CrossRef](#)]
27. Zhao, B.; Hiller, J.; Awada, T.; Wardlow, B.; Erickson, G.; Shi, Y. Forage biomass estimation using UAV-based remote sensing and machine learning: A tool for assessing management practices. *Ecol. Inf.* **2025**, *90*, 103361. [[CrossRef](#)]
28. Smith, W.B.; Galyean, M.L.; Kallenbach, R.L.; Greenwood, P.L.; Scholljegerdes, E.J. Understanding Intake on Pastures: How, Why, and a Way Forward. *J. Anim. Sci.* **2021**, *99*, skab062. [[CrossRef](#)] [[PubMed](#)]
29. Menendez, H.M., III. Improving Dry Matter Intake Estimates Using Precision Systems. *Animals* **2023**, *13*, 3844. [[CrossRef](#)] [[PubMed](#)]
30. Akdağ, A.; Ocağ, N. Herbage Intake Determination Methods of Grazing Animals. *Sci. Pap. Anim. Sci. Biotechnol.* **2019**, *52*, 3586–3603.
31. Agenzia Regionale per lo Sviuppo e i Servizi in Agricoltura. *I Suoli Della Calabria—Carta Dei Suoli in Scala 1:250.000*; Rubbettino Industrie Grafiche: Catanzaro, Italy, 2023.
32. Soil Survey Staff. *Keys to Soil Taxonomy*, 12th ed; USDA-Natural Resources Conservation Service: Washington, DC, USA, 2014.
33. Cilione, C.; Badagliacca, G.; Messina, G.; Praticò, S.; Modica, G.; Caparra, P. UAV-Based Pasture Characterization for Precision Grazing Management: Preliminary Results in Calabria (Southern Italy). In *International Workshop IFTToMM for Sustainable Development Goals*; Carbone, G., Quaglia, G., Eds.; Springer Nature: Cham, Switzerland, 2025; pp. 632–640.
34. Pellicone, G.; Caloiero, T.; Coletta, V.; Veltri, A. Phytoclimatic map of Calabria (Southern Italy). *J. Maps* **2014**, *10*, 109–113. [[CrossRef](#)]
35. Kjeldahl, J.G.C.T. Neue methode zur bestimmung des stickstoffs in organischen körpern. *Z. Für Anal. Chem.* **1883**, *22*, 366–382. [[CrossRef](#)]
36. AOAC International. *Official Methods of Analysis of AOAC International*, 16th ed.; AOAC International: Arlington, VA, USA, 1995.
37. Van Soest, P.J.; Robertson, J.B.; Lewis, B.A. Methods for dietary fiber, neutral detergent fiber, and nonstarch polysaccharides in relation to animal nutrition. *J. Dairy.Sci.* **1991**, *74*, 3583–3597. [[CrossRef](#)]
38. Undi, M.; Wilson, C.; Ominski, K.H.; Wittenberg, K.M. Comparison of techniques for estimation of forage dry matter intake by grazing beef cattle. *Can. J. Anim. Sci.* **2008**, *88*, 693–701. [[CrossRef](#)]
39. Badagliacca, G.; Messina, G.; Presti, E.L.; Preiti, G.; Di Fazio, S.; Monti, M.; Modica, G.; Praticò, S. Durum Wheat (*Triticum durum* Desf.) Grain Yield and Protein Estimation by Multispectral UAV Monitoring and Machine Learning Under Mediterranean Conditions. *AgriEngineering* **2025**, *7*, 99. [[CrossRef](#)]
40. Vincini, M.; Frazzi, E. Comparing narrow and broad-band vegetation indices to estimate leaf chlorophyll content in planophilecrop canopies. *Precis. Agric.* **2011**, *12*, 334–344. [[CrossRef](#)]
41. Cao, X.; Liu, Y.; Yu, R.; Han, D.; Su, B. A Comparison of UAV RGB and Multispectral Imaging in Phenotyping for Stay Green of Wheat Population. *Remote Sens.* **2021**, *13*, 5173. [[CrossRef](#)]
42. Gitelson, A.A.; Kaufman, Y.J.; Merzlyak, M.N. Use of a green channel in remote sensing of global vegetation from EOS-MODIS. *Remote Sens. Environ.* **1996**, *58*, 289–298. [[CrossRef](#)]
43. Haboudane, D.; Miller, J.R.; Pattey, E.; Zarco-Tejada, P.J.; Strachan, I.B. Hyperspectral vegetation indices and novel algorithms for predicting green LAI of crop canopies: Modeling and validation in the context of precision agriculture. *Remote Sens. Environ.* **2004**, *90*, 337–352. [[CrossRef](#)]

44. Rouse, J.W.; Haas, R.H.; Schell, J.A.; Deering, D.W. Monitoring vegetation systems in the Great Plains with ERTS. *Remote Sens. Environ.* **1974**, *1*, 127–135.
45. Baret, F.; Guyot, G. Potentials and limits of vegetation indices for LAI and APAR assessment. *Remote Sens. Environ.* **1991**, *35*, 161–173. [[CrossRef](#)]
46. Rouse, J.W.; Haas, R.H.; Schell, J.A.; Deering, D.W. Monitoring vegetation systems in the Great Plains with ERTS. In *Third Earth Resources Technology Satellite-1 Symposium*; NASA SP-351; NASA: Washington, DC, USA, 1974; Volume 1, pp. 309–317.
47. Gitelson, A.A.; Merzlyak, M.N. Remote sensing of chlorophyll concentration in higher plant leaves. *Remote Sens. Environ.* **1997**, *58*, 289–298. [[CrossRef](#)]
48. Qi, J.; Chehbouni, A.; Huete, A.R.; Kerr, Y.H.; Sorooshian, S. A modified soil adjusted vegetation index (MSAVI). *Remote Sens. Environ.* **1994**, *48*, 119–126. [[CrossRef](#)]
49. Gitelson, A.A.; Kaufman, Y.J.; Stark, R.; Rundquist, D. Novel algorithms for remote estimation of vegetation fraction. *Remote Sens. Environ.* **2002**, *80*, 76–87. [[CrossRef](#)]
50. Huete, A.R. A soil-adjusted vegetation index (SAVI). *Remote Sens. Environ.* **1988**, *25*, 295–309. [[CrossRef](#)]
51. R CoreTeam. *R: A Language and Environment for Statistical Computing*; R Foundation for Statistical Computing: Vienna, Austria, 2021.
52. Soetewey, A. Correlation Coefficient and Correlation Test in R-Stats and R. 2020, pp. 1–27. Available online: <https://statsandr.com/blog/correlation-coefficient-and-correlation-test-in-r/> (accessed on 15 September 2025).
53. Kuhn, M.; Wing, J.; Weston, S.; Williams, A. The caret package. *Gene Expr.* **2007**, *28*, 1–26.
54. Araújo, S.O.; Peres, R.S.; Ramalho, J.C.; Lidon, F.; Barata, J. machine learning applications in agriculture: Current trends, challenges, and future perspectives. *Agronomy* **2023**, *13*, 2976. [[CrossRef](#)]
55. Meshram, V.; Patil, K.; Meshram, V.; Hanchate, D.; Ramkteke, S.D. Machine learning in agriculture domain: A state-of-art survey. *Artif. Intell. Life Sci.* **2021**, *1*, 100010. [[CrossRef](#)]
56. Kuhn, M. Building Predictive Models in R Using the Caret Package. *J. Statistical Softw.* **2008**, *28*, 1–262. [[CrossRef](#)]
57. Pysillos, G.; Hadjigeorgiou, I.; Dimitrakopoulos, P.G.; Kizos, T. Grazing Land Productivity, Floral Diversity, and Management in a Semi-Arid Mediterranean Landscape. *Sustainability* **2022**, *14*, 4623. [[CrossRef](#)]
58. Serrano, J.; Shahidian, S.; Moral, F.; Carvajal-Ramirez, F.; Marques da Silva, J. Estimation of Productivity in Dryland Mediterranean Pastures: Long-Term Field Tests to Calibration and Validation of the Grassmaster II Probe. *AgriEngineering* **2020**, *2*, 240–255. [[CrossRef](#)]
59. Serrano, J.; Franco, J.; Shahidian, S.; Moral, F.J. Estimation of Dry Matter Yield in Mediterranean Pastures: Comparative Study between Rising Plate Meter and Grassmaster II Probe. *Agriculture* **2024**, *14*, 1737. [[CrossRef](#)]
60. Hadjigeorgiou, I.; Osoro, K.; Fragoso de Almeida, J.P.; Molle, G. Southern European grazing lands: Production, environmental and landscape management aspects. *Livest. Prod. Sci.* **2005**, *96*, 51–59. [[CrossRef](#)]
61. Orlandi, S.; Probo, M.; Sitzia, T.; Trentanovi, G.; Garbarino, M.; Lombardi, G.; Lonati, M. Environmental and land use determinants of grassland patch diversity in the western and eastern Alps under agro-pastoral abandonment. *Biodivers. Conserv.* **2016**, *25*, 275–293. [[CrossRef](#)]
62. Bellini, E.; Martin, R.; Argenti, G.; Staglianò, N.; Costafreda-Aumedes, S.; Dibari, C.; Moriondo, M.; Bellocchi, G. Opportunities for Adaptation to Climate Change of Extensively Grazed Pastures in the Central Apennines (Italy). *Land* **2023**, *12*, 351. [[CrossRef](#)]
63. Xie, K.; Liu, F.; Zhang, C.; Hou, F. Nitrogen and energy utilization and methane emissions of sheep grazing on annual pasture vs. native pasture. *J. Anim. Sci.* **2024**, *102*, skae032. [[CrossRef](#)] [[PubMed](#)]
64. Lin, L.; Dickhoefer, U.; Muller, K.; Wurina; Susenbeth, A. Grazing behavior of sheep at different stocking rates in the Inner Mongolian steppe, China. *Appl. Anim. Nutr.* **2011**, *129*, 36–42. [[CrossRef](#)]
65. Piasentier, E.; Saccà, E.; Bovolenta, S. Dietary selection and ingestive behaviour of fallow deer and sheep grazing on adjacent monocultures of white clover and tall fescue. *Small Rumin. Res.* **2007**, *71*, 222–233. [[CrossRef](#)]
66. Tlahig, S.; Neji, M.; Atoui, A.; Seddik, M.; Dbara, M.; Yahia, H.; Nagaz, K.; Najari, S.; Khorchani, T.; Loumerem, M. Genetic and seasonal variation in forage quality of lucerne (*Medicago sativa* L.) for resilience to climate change in arid environments. *J. Agric. Food Res.* **2024**, *15*, 100986. [[CrossRef](#)]
67. Edouard, N.; Fleurance, G.; Martin-Rosset, W.; Duncan, P.; Dulphy, J.P.; Grange, S.; Baumont, R.; Dubroeuq, H.; Pérez-Barbería, F.J.; Gordon, I.J. Voluntary intake and digestibility in horses: Effect of forage quality with emphasis on individual variability. *Animal* **2008**, *2*, 1526–1533. [[CrossRef](#)]
68. Serrano, J.; Roma, L.; Shahidian, S.; Belo, A.; Carreira, E.; Paniagua, L.L.; Moral, F.; Paixão, L.; Marques da Silva, J. A technological approach to support extensive livestock management in the portuguese Montado ecosystem. *Agronomy* **2022**, *12*, 1212. [[CrossRef](#)]
69. Wróbel, B.; Zielewicz, W.; Paszkiewicz-Jasińska, A. Improving forage quality from permanent grasslands to enhance ruminant productivity. *Agriculture* **2025**, *15*, 1438. [[CrossRef](#)]

70. Bacchi, M.; Monti, M.; Calvi, A.; Lo Presti, E.; Pellicanò, A.; Preiti, G. Forage potential of cereal/legume intercrops: Agronomic performances, yield, quality forage and LER in two harvesting times in a Mediterranean environment. *Agronomy* **2021**, *11*, 121. [[CrossRef](#)]
71. Togeiro de Alckmin, G.; Kooistra, L.; Rawnsley, R.; Lucieer, A. Comparing methods to estimate perennial ryegrass biomass: Canopy height and spectral vegetation indices. *Precis. Agric.* **2021**, *22*, 205–225. [[CrossRef](#)]
72. Sangjan, W.; Carpenter-Boggs, L.A.; Hudson, T.D.; Sankaran, S. Pasture productivity assessment under mob grazing and fertility management using satellite and UAS imagery. *Drones* **2022**, *6*, 232. [[CrossRef](#)]
73. Fern, R.R.; Foxley, E.A.; Bruno, A.; Morrison, M.L. Suitability of NDVI and OSAVI as estimators of green biomass and coverage in a semi-arid rangeland. *Ecol. Indic.* **2018**, *94*, 16–21. [[CrossRef](#)]
74. Wijesingha, J.; Astor, T.; Schulze-Brüninghoff, D.; Wengert, M.; Wachendorf, M. Predicting forage quality of grasslands using UAV-borne imaging spectroscopy. *Remote Sens.* **2020**, *12*, 126. [[CrossRef](#)]
75. Sánchez, N.; Plaza, J.; Pouyez, L.; Palacios, C. Estimation of forage yield using the second derivative of Normalized Difference Vegetation Index time series from Sentinel-2. *Grass Forage Sci.* **2025**, *80*, e70008. [[CrossRef](#)]
76. Wang, F.; Yang, M.; Ma, L.; Zhang, T.; Qin, W.; Li, W.; Zhang, Y.; Sun, Z.; Wang, Z.; Li, F.; et al. Estimation of above-ground biomass of winter wheat based on consumer-grade multi-spectral UAV. *Remote Sens.* **2022**, *14*, 1251. [[CrossRef](#)]
77. Porter, T.F.; Chen, C.; Long, J.A.; Lawrence, R.L.; Sowell, B.F. Estimating biomass on CRP pastureland: A comparison of remote sensing techniques. *Biomass Bioenergy* **2014**, *66*, 268–274. [[CrossRef](#)]
78. Serrano, J.; Shahidian, S.; Paixão, L.; Marques da Silva, J.; Paniágua, L.L. Pasture quality assessment through NDVI obtained by remote sensing: A validation study in the Mediterranean silvo-pastoral ecosystem. *Agriculture* **2024**, *14*, 1350. [[CrossRef](#)]
79. Carneiro, F.M.; Angeli Furlani, C.E.; Zerbato, C.; de Menezes, P.C.; da Silva Gírio, L.A.; de Oliveira, M.F. Comparison between vegetation indices for detecting spatial and temporal variabilities in soybean crop using canopy sensors. *Precis. Agric.* **2020**, *21*, 979–1007. [[CrossRef](#)]
80. Gao, S.; Zhong, R.; Yan, K.; Ma, X.; Chen, X.; Pu, J.; Gao, S.; Qi, J.; Yin, G.; Myneni, R.B. Evaluating the saturation effect of vegetation indices in forests using 3D radiative transfer simulations and satellite observations. *Remote Sens. Environ.* **2023**, *295*, 113665. [[CrossRef](#)]
81. de Almeida, S.L.H.; Souza, J.B.C.; Nogueira, S.F.; Pezzopane, J.R.M.; Teixeira, A.H.d.C.; Bosi, C.; Adami, M.; Zerbato, C.; Bernardi, A.C.d.C.; Bayma, G.; et al. Forage mass estimation in silvopastoral and full sun systems: Evaluation through proximal remote sensing applied to the SAFER model. *Remote Sens.* **2023**, *15*, 815. [[CrossRef](#)]
82. Serrano, J.; Mendes, S.; Shahidian, S.; Marques da Silva, J. Pasture quality monitoring based on proximal and remote optical sensors: A case study in the Montado Mediterranean ecosystem. *AgriEngineering* **2023**, *5*, 380–394. [[CrossRef](#)]
83. Barnes, P.; Wilson, B.R.; Reid, N.; Bayerlein, L.; Koen, T.B.; Olupot, G. Examining the impact of shade on above-ground biomass and normalized difference vegetation index of C₃ and C₄ grass species in North-Western NSW, Australia. *Grass Forage Sci.* **2015**, *70*, 324–334. [[CrossRef](#)]
84. Barnetson, J.; Phinn, S.; Scarth, P. Estimating plant pasture biomass and quality from UAV imaging across Queensland's rangelands. *AgriEngineering* **2020**, *2*, 523–543. [[CrossRef](#)]
85. Geipel, J.; Bakken, A.K.; Jørgensen, M.; Korsæth, A. Forage yield and quality estimation by means of UAV and hyperspectral imaging. *Precis. Agric.* **2021**, *22*, 1437–1463. [[CrossRef](#)]
86. Zhou, X.; Kono, Y.; Win, A.; Matsui, T.; Tanaka, T.S.T. Predicting within-field variability in grain yield and protein content of winter wheat using UAV-based multispectral imagery and machine learning approaches. *Plant Prod. Sci.* **2021**, *24*, 137–151. [[CrossRef](#)]
87. Filippi, P.; Whelan, B.M.; Vervoort, R.W.; Bishop, T.F.A. Mid-season empirical cotton yield forecasts at fine resolutions using large yield mapping datasets and diverse spatial covariates. *Agric. Syst.* **2020**, *184*, 102894. [[CrossRef](#)]
88. Shendryk, Y.; Davy, R.; Thorburn, P.J. Integrating satellite imagery and environmental data to predict field-level cane and sugar yields in Australia using machine learning. *Field Crops Res.* **2020**, *260*, 107984. [[CrossRef](#)]
89. Montesinos López, O.A.; Montesinos López, A.; Crossa, J. Support Vector Machines and Support Vector Regression. In *Multivariate Statistical Machine Learning Methods for Genomic Prediction*; Springer International Publishing: Cham, Switzerland, 2022; pp. 337–378. [[CrossRef](#)]
90. Castillo-Girones, S.; Munera, S.; Martínez-Sober, M.; Blasco, J.; Sanmillan Blasco, J.L.; Cubero, S.; Gómez-Sanchís, J. Artificial Neural Networks in Agriculture, the core of artificial intelligence: What, When, and Why. *Comput. Electron. Agric.* **2025**, *230*, 109938. [[CrossRef](#)]
91. Leo, S.; De Antoni Migliorati, M.; Grace, P.R. Predicting within-field cotton yields using publicly available datasets and machine learning. *Agron. J.* **2021**, *113*, 1150–1163. [[CrossRef](#)]
92. Adar, S.; Sternberg, M.; Paz-Kagan, T.; Henkin, Z.; Dovrat, G.; Zaady, E.; Argaman, E. Estimation of aboveground biomass production using an unmanned aerial vehicle (UAV) and VEN μ S satellite imagery in Mediterranean and semiarid rangelands. *Remote Sens. Appl. Soc. Environ.* **2022**, *26*, 100753. [[CrossRef](#)]

93. Belgiu, M.; Drăguț, L. Random forest in remote sensing: A review of applications and future directions. *ISPRS J. Photogramm. Remote Sens.* **2016**, *114*, 24–31. [[CrossRef](#)]
94. Alvarez-Mendoza, C.I.; Guzman, D.; Casas, J.; Bastidas, M.; Polanco, J.; Valencia Ortiz, M.; Montenegro, F.; Arango, J.; Ishitani, M.; Selvaraj, M. Predictive Modeling of Above-Ground Biomass in Brachiaria Pastures from Satellite and UAV Imagery Using Machine Learning Approaches. *Remote Sens.* **2022**, *14*, 5870. [[CrossRef](#)]
95. Wang, X.; Yan, S.; Wang, W.; Yin, L.; Liubing, Y.; Li, M.; Yu, Z.; Chang, S.; Hou, F. Monitoring leaf area index of the sown mixture pasture through UAV multispectral image and texture characteristics. *Comput. Electron. Agric.* **2023**, *214*, 108333. [[CrossRef](#)]
96. Pullanagari, R.R.; Kereszturi, G.; Yule, I.J. Integrating airborne hyperspectral, topographic, and soil data for estimating pasture quality using recursive feature elimination with random forest regression. *Remote Sens.* **2018**, *10*, 1117. [[CrossRef](#)]
97. Mas, J.F.; Flores, J.J. The application of artificial neural networks to the analysis of remotely sensed data. *Int. J. Remote Sens.* **2008**, *29*, 617–663. [[CrossRef](#)]
98. Mutanga, O.; Skidmore, A.K. Integrating imaging spectroscopy and neural networks to map grass quality in the Kruger National Park, South Africa. *Remote Sens. Environ.* **2004**, *90*, 104–115. [[CrossRef](#)]
99. Liu, H.; Zhu, H.; Li, Z.; Yang, G. Quantitative analysis and hyperspectral remote sensing of the nitrogen nutrition index in winter wheat. *Int. J. Remote Sens.* **2020**, *41*, 858–881. [[CrossRef](#)]
100. Yue, J.; Feng, H.; Yang, G.; Li, Z. A comparison of regression techniques for estimation of above-ground winter wheat biomass using near-surface spectroscopy. *Remote Sens.* **2018**, *10*, 66. [[CrossRef](#)]
101. Alvarez-Hess, P.S.; Thomson, A.L.; Karunaratne, S.B.; Douglas, M.L.; Wright, M.M.; Auld, M.J. Using multispectral data from an unmanned aerial system to estimate pasture depletion during grazing. *Anim. Feed Sci. Technol.* **2021**, *275*, 114880. [[CrossRef](#)]

Disclaimer/Publisher’s Note: The statements, opinions and data contained in all publications are solely those of the individual author(s) and contributor(s) and not of MDPI and/or the editor(s). MDPI and/or the editor(s) disclaim responsibility for any injury to people or property resulting from any ideas, methods, instructions or products referred to in the content.